Chemical and Materials Engineering 2(8): 179-189, 2014
DOI: 10.13189/cme.2014.020803 http://www.hrpub.org

Surface Characteristics of Silicon Nitride Compounds Deposited on Plasma Nitrided Austenitic Stainless Steels 316L

Ahmad Reza Rastkar*, Sepehrdad Akbari

Laser and Plasma Research Institute, Shahid Beheshti University, Tehran 1983969411, Iran

Abstract Silicon nitride compound deposited by plasma enhanced chemical vapor deposition (PECVD) on plasma nitrided stainless steel 316L using tetraethylorthosilicate (TEOS):H_2:N_2 mixtures. Plasma nitriding is extensively used to improve the hardness and wear performance of steels. It is also known that silicon nitride compounds can have interesting properties, such as low friction coefficient, high hardness and wear resistance. Therefore the deposition processes were carried out at optimized gas compositions and temperatures in order to obtain a combination of the best mechanical and enhanced tribological properties. The composition and structure of the surface layers were characterized using XRD, Glancing angle X-ray diffraction (GAXRD), optical and EDX built in electron microscopy, Microhardness and pin-on-disc wear tests. The compound of α-Si_3N_4 was found on the top surfaces of PECVD and plasma nitrided austenitic stainless steel 316 L. The nitride compounds were composed of $Fe_{2-3}N$, Fe_4N in addition to chromium nitride. PECVD treatments substantially improved the hardness and wear resistance of plasma nitrided SS 316 L and reduced the friction coefficient and wear rate of the samples. The investigation showed that the combination of PECVD of organosilicon compounds and plasma nitriding results in superior high hardness, low friction and high wear resistance of treated surfaces if compared to those of conventional plasma nitrided surfaces.

Keywords PECVD, α-Si_3N_4, Friction, Hardness, Plasma Nitriding

1. Introduction

In recent years, the treatment of surfaces with oxides and nitrides has increasingly gained importance in wear resistant applications. Anti-abrasion layers are necessary to increase the hardness and improve the resistance of surface against strokes, impacts of small particles and large pieces as well as friction. Industries use stainless steels for the good corrosion resistant and toughness of these materials where contact pressures are not considerable [1-2]. The high demand for these alloys requires the improvement of their surface hardness and wear resistance.

Nitriding improves the surface hardness and wear resistance of various steel materials, such as tool steels and stainless steels. Thermo-chemical diffusion treatments such as nitriding and carburizing processes alter the surface of austenitic stainless steels as a main group of these materials [3-6]. However, the investigators carry out nitriding merely at low temperatures using liquid, gas or plasma environments; the industry is being more interested in plasma nitriding over traditional gas and bath nitriding [7-9].

Plasma technology reduces gas and energy consumption and the complete removal of environmental hazards. Plasma nitriding at temperatures around 500 °C can produce thick nitride compound layers on austenitic stainless steels [3-8].

Silicon nitride coatings are more investigated in the industry of integrated circuits. However, a compound such as silicon nitride (α-Si_3N_4) coating has a considerable potential for industrial applications due to their high temperature solid lubricating, high hardness and strength and high wear-resistance [10-13]. It has been found that some low pressure plasma deposited silicon nitride, oxide and oxynitride compounds can sustain compression stress up to 50 MPa [14].

Therefore silicon nitride (α- Si_3N_4) can be used on the top of nitrided surfaces as a load bearing material. Vapor-solid thermal reaction of ammonia and silicon monoxide, via catalyst-assisted pyrolysis of polymeric precursors and plasma enhanced chemical vapor deposition (PECVD) of organosilicon compounds can deposit silicon nitride (α-Si_3N_4).

TEM and XRD studies have shown that α- Si_3N_4, β-SiC and amorphous silicon oxide separate from the SiCN layers at high temperature [15]. The quality and properties of deposited coatings depend on the relative contributions, reactions and cracking of neutral active species as well as ions under plasma conditions [16, 17]. Also it has been found that the methyl groups are removed from organosilicon

compounds and $Si(CH_3)_3$ ions by cracking the Si–O bonds as the dominant dissociation channels resulting in other bonds [18].

Therefore it would be possible to produce α-Si_3N_4 from silicon containing organometallic compounds at high electron temperatures of cold plasma deposition processes. In this study the combined effect of PECVD of silicon nitride from TEOS:H_2:N_2 gas mixture and plasma nitriding was investigated on the microstructure and tribomechanical properties of austenitic stainless steel 316 L.

2. Experimental Methods and Material

Austenitic stainless steel 316 L was the substrate in this study. The specimens were cut from 25 mm bar shape material in 5 mm thickness. The samples grinded by emery papers up to 1500 mesh and cleaned in alcohol and acetone before placing in the vacuum chamber.

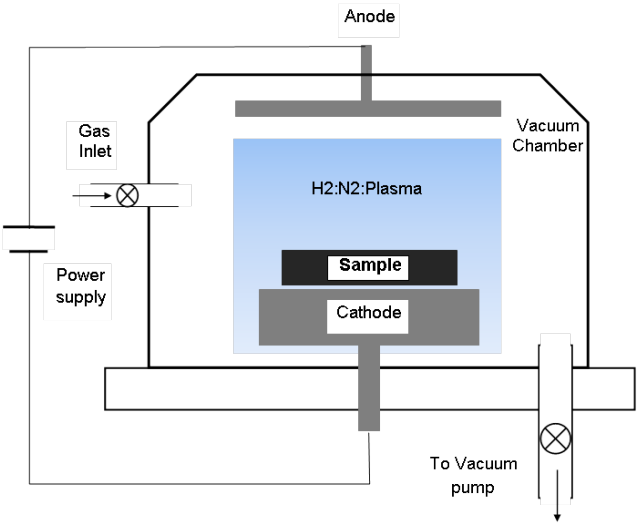

Figure 1. The apparatus for plasma nitriding and PECVD treatments.

Before plasma nitriding, the samples cleaned via sputtering in the plasma reactor by application a gas mixture of 50% Ar 50% H_2 for 1 h to remove any passive film on the surface of stainless steel. This mixture combines the mechanical removal action of Ar and the reducing effect of hydrogen on Cr_2O_3. The apparatus for plasma nitriding and PECVD treatments was laboratory type working with pulsed D.C. power source at a frequency of 18 kHz (Figure 1).

The treatments were carried out at 10 mbar working pressure and different voltages to achieve the cathode (substrate) temperature (nitriding temperature) up to 500 °C. The PECVD of silicon nitrides compounds were carried out at different temperatures and times using tetraethylorthosilicat (TEOS) as a precursor of silicon in the gas mixtures of nitrogen and hydrogen (Table 1).

X-ray diffraction (XRD) and glancing angle X-ray diffraction (GAXRD) were undertaken to identify the phases formed during plasma treatments. The GAXRD spectra were obtained at fixed incident angles of 1° and 9°. Optical microscope (OM) and energy dispersive X-ray spectrometry (EDX) built in scanning electron microscope (SEM) were used to analyze the compound layers.

Vickers microhardness values obtained at different loads. Atomic force microscopy (AFM, Nanosurf II) was used to examine the morphology and roughness of plasma treated surfaces. AFM imaging was performed in contact mode with V-shaped cantilevers (spring constant between 0.1 and 0.02 N/m).

Pin-on-disk configuration was used to evaluate the friction coefficient and wear rates in dry air at room temperature without lubrication. The specimens were cooled in nitrogen atmosphere after treatments.

A normal load of 10 N was applied to the pin of chromium steel 52100 with a tip diameter of 6 mm as the counterpart material at a sliding speed of 10 mm/s. The friction coefficient (μ) was recorded during the test and the wear rate (K) was measured after 300 m using the formula $K=V/(F\times s)$, where V is the worn volume, F is the normal load, and s is the sliding distance.

The worn volume was calculated from multiplication of the depth, width and diameter of the wear tracks. A surface profilometer (DEKTAK 8000) determined the values. The diameter of the wear tracks was 20 mm. Tests were interrupted at regular intervals of sliding distances in order to monitor the mass loss.

Table 1. Experimental conditions of typical plasma nitriding and PECVD treatments on stainless steel 316L samples.

Treatment	Temperature (°C)	Time (h)	H_2:N_2 gas ratio	Tetraethylorthosilicate (TEOS) (sccm)	Voltage (volts)
Plasma nitriding	500	1.5	1:3	-	- 600
Plasma nitriding	500	3	1:3	-	- 600
Plasma nitriding	500	5	1:3	-	- 600
PECVD after 1.5 h Plasma nitriding	400	1.5	1:3	10	-450
PECVD after 3 h Plasma nitriding	400	1.5	1:3	10	-450
PECVD after 5 h Plasma nitriding	400	1.5	1:3	10	-450

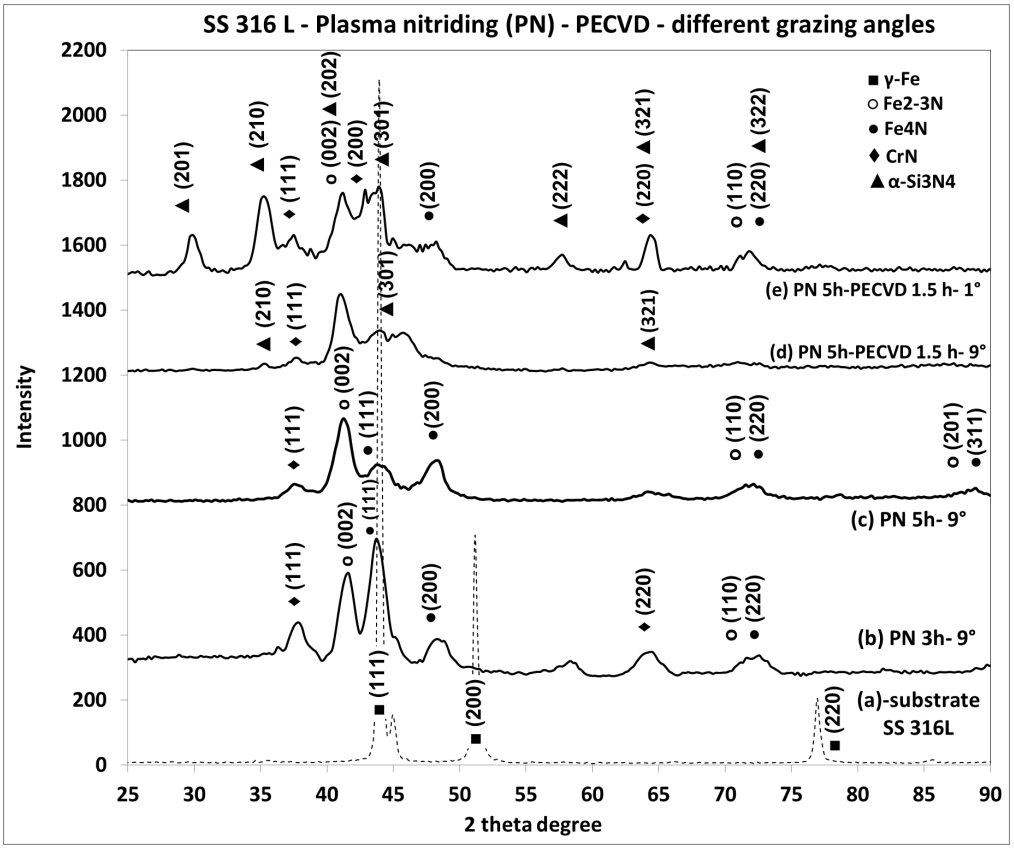

Figure 2. (a) XRD spectrum of untreated SS 316L, GAXRD spectra of (b) SS 316L plasma nitrided for 3 h at 500 °C in H_2:N_2=1:3 gas mixture at glancing angle of 9 degree, (c) SS 316L plasma nitrided for 5 h at 500 °C in H_2:N_2=1:3 gas mixture at glancing angle of 9 degree, (d) SS 316L deposited by PECVD of silicon nitride at 400 °C for 1.5 h by the addition of 10 sccm tetraethylorthosilicate (TEOS) to the H_2:N_2=1:3 gas mixture after plasma nitriding at glancing angle of 9 degree and (e) the (d) treatment at glancing angle of 1 degree.

3. Results and Discussion

3.1. Identification of Nitride and Silicon Nitride Phases

The XRD pattern of untreated 316L stainless steel and typical treatments is shown in Figure 2. The XRD pattern of untreated 316L stainless steel shows a typical austenite phase (γ-austenite) in Figure 2a. Plasma nitriding of all samples was performed at 500 °C and resulted in the formation $Fe_{2-3}N$ and Fe_4N and CrN compounds on the surface.

These results can be explained by the diffusion mechanisms of nitrogen and chromium. That is, at 500 °C, the nitrides like CrN, $Fe_{2-3}N$ and Fe_4N form due to partial decomposition of the metastable supersaturated austenite phase [19].

The XRD pattern in Figure 2b was taken at 9 degree glancing angle to show the intensity of the nitride peaks as much as possible, as the nitride layers showed a low intensity at normal incidence of XRD test due to the rather low thickness of the layers. The intensity of γ-austenite peaks decreased and nitride peaks appeared clearly in the pattern (Figure 2b).

It has been shown by glancing angle XRD that CrN precipitations can be seen in the plasma nitriding conditions at temperatures above 460 °C with the gas mixtures containing more than 10% N_2 gas. Otherwise, the S-phase (expanded austenite, γ_N) is observed in the microstructure [20]. The S-phase peaks disappear at temperatures higher than 460 °C.

In fact at higher temperatures the solubility of nitrogen in the austenitic structure is exceeded and the metastable S-phase decomposes and the precipitation of CrN occurs [21]. Also XPS studies report the evolution of the atomic fraction of different components contributing to both Cr2p and Fe2p lines as a function of nitriding time. In both cases, it has been observed that the surface composition is stabilized after approximately 3 h of nitriding and the overall hydroxyl species are affected by the nitriding process.

The results have suggested the formation of chromium nitride (CrN) and iron nitrided species. Therefore, it has been concluded that plasma nitriding leads to surface reduction, mainly by removing hydroxyl species, and to the formation of nitrided compounds [22]. The intensity of Fe_4N (111) peak decreases and the intensity of $Fe_{2-3}N$ (002) peak increases after 5 h plasma nitriding (Figure 2c). This is an indication of nitrogen diffusion across the nitride layers into the substrate and formation of $Fe_{2-3}N$ with lower nitrogen from nitrides such as Fe_4N with higher nitrogen.

Addition of TEOS vapor to the gas mixture after 5 h plasma nitriding resulted in the formation of silicon nitride

compound on the top surface (Figure 2d and Figure 2e). Different compounds of silicon, nitrogen and oxygen were investigated for the best matching with the peaks appeared in the XRD spectrum.

It was found that α-Si_3N_4 was the most probable compound on the surface of the two steps treated surfaces. The structural complexity of silicon nitride is less diverse and only two polymorphs, α- and β- Si_3N_4, are known at ambient conditions. Both structures consist of Si atoms tetrahedrally coordinated by four N atoms.

By initiating the process, silicon is quickly converted to silicon nitride phase through a highly favorable and exothermic reaction [23-25].

Therefore it can be proposed that TEOS in N_2 atmosphere has been dissociated to Si and combusted to SiO_2 and Si_3N_4 compounds. It can also be stated that the necessary heat to initiate these reactions is provided by the high electron temperatures in the plasma sheaths in front of the samples surfaces. Furthermore the existence of active hydrogen species, could remove the residual oxide layer chemically from the nitrided surface during PECVD process.

Consequently silicon nitride is the most probable phase presented in the surface layers [26-27]. The above postulation of formation of nitride phases can be observed in the XRD pattern of PECVD treated layers which show silicon nitride (α-Si_3N_4) (Figure 2d and Figure 2e) in addition to iron nitride phases of $Fe_{2-3}N$, Fe_4N and CrN. To assure the existence of α-Si_3N_4 phase on top of the nitride phases of $Fe_{2-3}N$ and Fe_4N, XRD experiments of two step treated surfaces were carried out at 9 degree (Figure 2d) and 1 degree (Figure 2e) glancing incidence angles. In glancing angles X-ray is merely diffracted from the top surface layers and shows the compounds on the top surface rather than the compounds in a greater depth. The peaks of (201) and (210) for α-Si_3N_4 appeared much stronger at 1 degree glancing incidence angle (Figure 2e), which were not clearly observable in 9 degree glancing incidence angle (Figure 2d).

However the intensity of $Fe_{2-3}N$ and Fe_4N peaks were significantly weaker than that of α-Si_3N_4 phase [28-30].

3.2. Microstructural Analysis

Some typical micrographs of the cross sections of plasma nitrided and PECVD treated samples are reported in Figure 3. After etching, the compound layers appear to be distinguishable from the substrate separated by a strong etched line (Figure 3). It should be noted that there is no obvious diffusion zone at the interface of the compound layers and stainless steel substrate. The concentration of nitrogen decreased slightly from the surface to the substrate until decreased suddenly at the interface indicating the absence of a reasonable diffusion zone. PECVD of TEOS:H_2:N_2 after plasma nitriding varied the surface layers and produced new phases in the top layers.

The topmost layers consisted of α-Si_3N_4 with different feature from the nitride layer. However the top layer after the two step treatment is thinner than the nitride layers (Figure 3c and 3d). The thinning of the layer is attributed to the sputtering and evaporation phenomena from the surface during PECVD process.

EDX analysis across the PECVD treated surface layers revealed considerable silicon element confirming the existence of silicon compound. EDX analysis on the external surface of the sample plasma nitrided for 5 h did not show any significant amount of silicon element (Figure 3e). While the PECVD treated surface layer of this sample revealed strong indication of silicon nitride (Figure 3f). Therefore it is strongly suggested that the top surface layer of PECVD treatment is a mixture of fine grained α-Si_3N_4 compound.

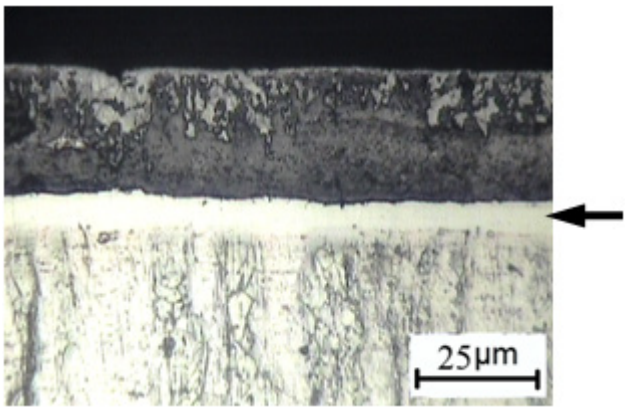

(a)

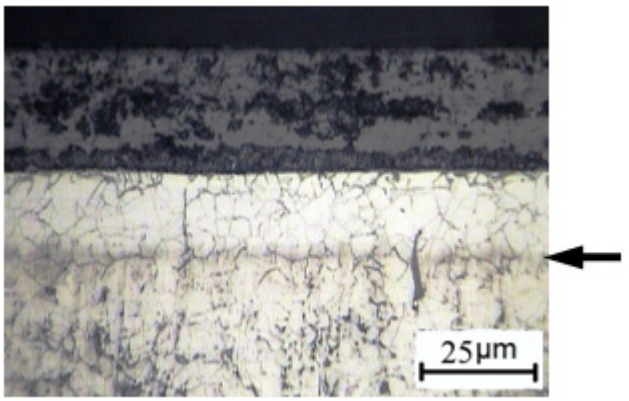

(b)

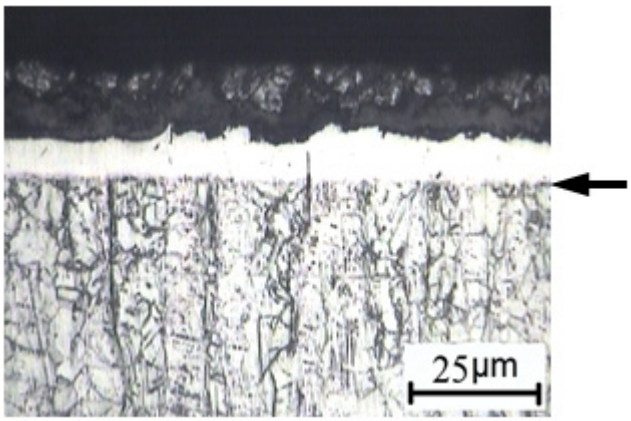

(c)

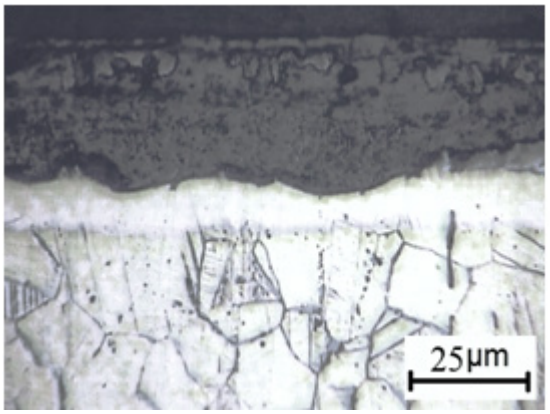

(d)

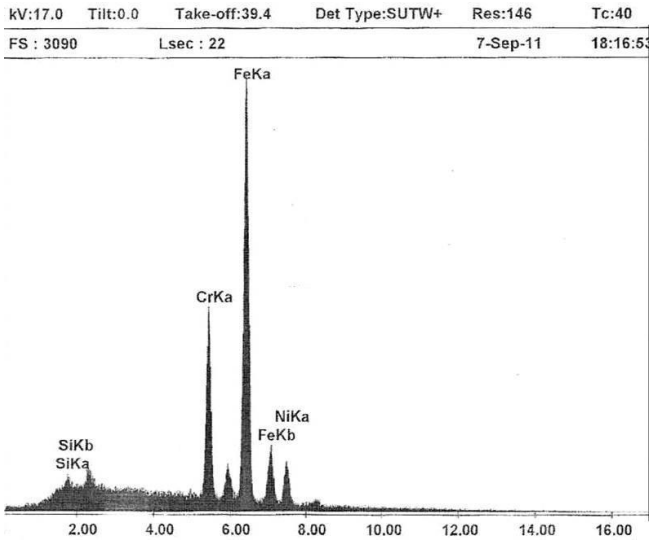

(e)

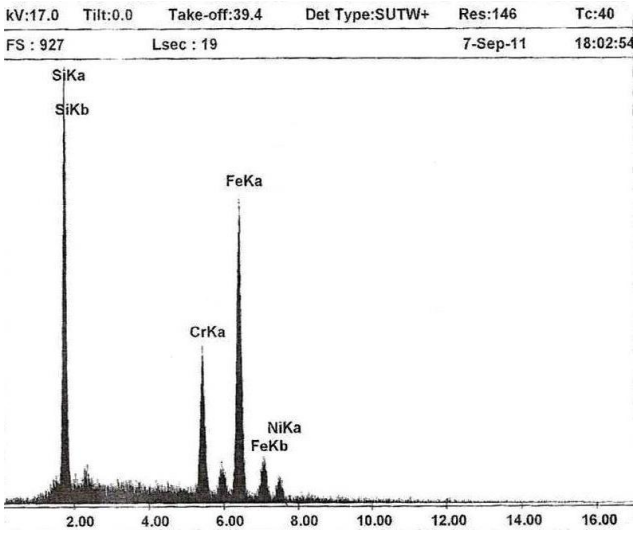

(f)

Figure 3. Optical micrographs of typical stainless steel 316 L samples plasma nitrided at 500 °C for (a) 3 h and (b) 5 h in H_2:N_2=1:3 gas mixture and the samples treated by PECVD of silicon nitride at 400 °C for 1.5 h by the addition of 10 sccm tetraethylorthosilicate (TEOS) to the H_2:N_2=1:3 gas mixture after (c) 3 h and (d) 5 h plasma nitriding. The arrows show the strong etched lines in the micrographs. The EDX analysis on the external surface of (b) and (d) are shown in (e) and (f) respectively.

3.3. Microhardness Evaluations

Figure 4 shows the surface microhardness value, measured at an applied load of 100 gf, for all selected samples. The surface microhardness value of all treated samples was several times more than that of untreated substrate (230 HV0.1). The higher surface microhardness of the two steps treated layers is attributed to the combination of hardness of hard nitride phases of $Fe_{2-3}N$, Fe_4N and CrN with silicon nitride (α-Si_3N_4) phases. It has been found that the surface hardness of such two steps treated samples is improved with respect to the hardness of underlying nitride layers [31]. The surface hardness of the two steps treated samples significantly increased with increasing the time of PECVD of TEOS at a flow rate of 10 sccm until 1.5 h to a maximum value of 2300 HV0.1.

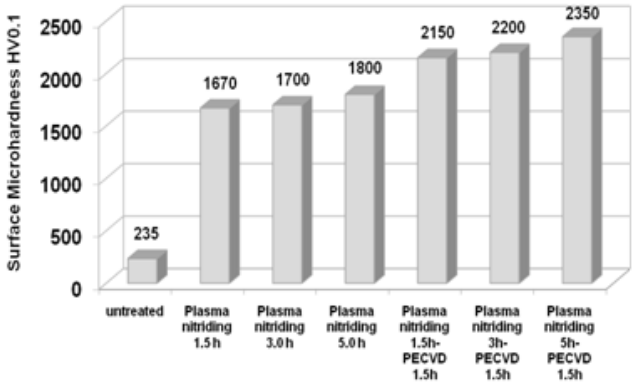

Figure 4. Surface microhardness of untreated stainless steel 316 L, plasma nitrided samples at 500 °C in H_2:N_2=1:3 gas mixture for different times and the samples treated by PECVD of silicon nitride at 400 °C for 1.5 h by the addition of 10 sccm tetraethylorthosilicate (TEOS) to the H_2:N_2=1:3 gas mixture after different times of plasma nitriding.

After that it decreased gradually with increasing the time. By increasing the PECVD time the top surface layers become thinner due to the counteracting removal action of the sputtering phenomenon during the deposition process. Therefore the thinner layers show a less hardness value than that of thicker layers. The surface hardness value of PECVD treated samples is approximately more than 1.2 and 10 times the associated values of untreated substrate and plasma nitrided samples, respectively. This high hardness and other characteristics then give rise to enhanced tribological properties as described in the following sections.

The hardness values of nitrided and PECVD treated samples are a combination of the hardness of the surface layers and the substrate due to the extra depth of indention. This behavior is common and thus it is widely accepted that the hardness of a coating measured by indentations is reliable with penetration depths not exceeding 5–10% of the total coating thickness, where substrate effects are negligible. A real hardness value of the surface layer should be examined with an indentation depth not exceeding one tenth of the surface layers.

In this study, it was not possible to obtain precise indentation impression with loads less than 100 gf due to the

distorted small size of the impressions. The real hardness values of the similar surfaces which nitrided and deposited by hard phases have been evaluated by nanoindentation. It has been found that after 3 h of nitriding, the hardness value exhibited a maximum of 14 GPa for indentation depths between approximately 50 and 125 nm in 2 µm thickness.

For indentation depths higher than 125 nm, the measurements were influenced by the stainless steel bulk material [22, 32-33]. Therefore the real surface hardness value of treated samples must be higher than those measured at load of 100 gf. Microhardness measurements at loads less than 100 gf were unreliable and were not reported until nanoindentation measurements are carried out in another study. The microhardness profile across the surface layers of most plasma nitrided (Figure 5a) and merely PECVD treated samples (Figure 5(b)) showed a considerable decrease in the values after a certain depth in the layers.

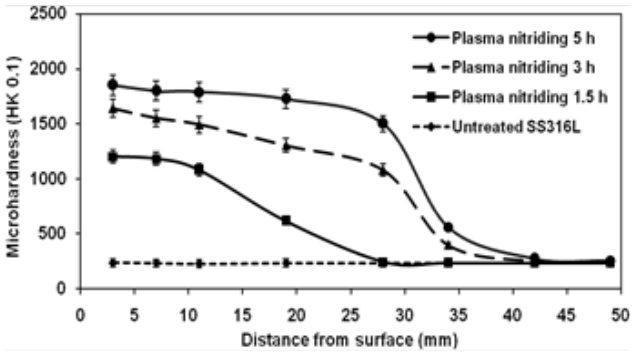

(a)

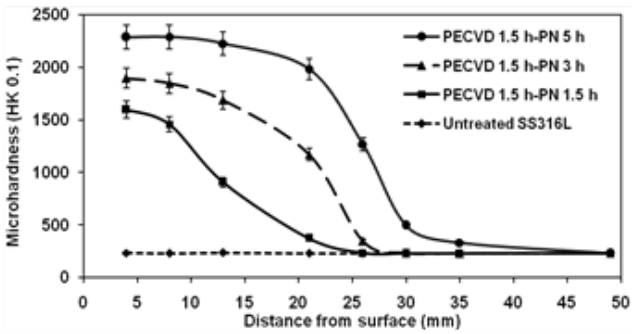

(b)

Figure 5. Microhardness across the surface layers of untreated stainless steel 316 L and (a) plasma nitrided samples at 500 °C in H_2:N_2=1:3 gas mixture for different times and (b) the samples treated by PECVD of silicon nitride at 400 °C for 1.5 h by the addition of 10 sccm tetraethylorthosilicate (TEOS) to the H_2:N_2=1:3 gas mixture after different times of plasma nitriding.

Microhardness values between 1700 and 2300 HV0.1 in the surface layers decreased to 230 HV which was the microhardness value of the substrate. This decrease of the hardness value is attributed to the absence of a considerable thick diffusion layer and a sharp interface between the compound layers and substrates. However this sharp interface did not affect the wear performance and load bearing capacity of the surface layers and no discontinuity was observed between the compound layers and substrates after deposition and mechanical tests.

3.4. Morphological Analysis

Figure 6 shows three-dimensional AFM images of typical surface morphology of untreated, plasma nitrided and PEVCD treated samples within an area of 50 µm × 50 µm.

The surface of untreated stainless steel 316 L clearly shows the grinding marks (Figure 6a), while the plasma nitriding and treatment resulted in different "mountain-like" morphologies (Figure 6b and 6c). This morphology can be ascribed to both the cathodic sputtering in both nitriding and PEVCD treatments [34]. In both cases sputtering phenomenon increases the surface roughness. However, it seems that the application of tetraethylorthosilicate (TEOS) which is dissociated to several radicals compensate the sputtering effect of nitrogen and hydrogen (Figure 6b), because these radicals are redeposited on the surface and make it smoother (Figure 6c). Moreover, these radicals create α-Si_3N_4 phase which are essentially low friction materials due to their low roughness [35-36]. The average surface area (Sa) and peak to peak surface area (Sy) roughness increased to 267.5 and 2374 nm respectively for the sample plasma nitrided for 5 h. While Sa and Sy increased to 136.1 and 1128.4 nm for the same sample after PECVD treatment.

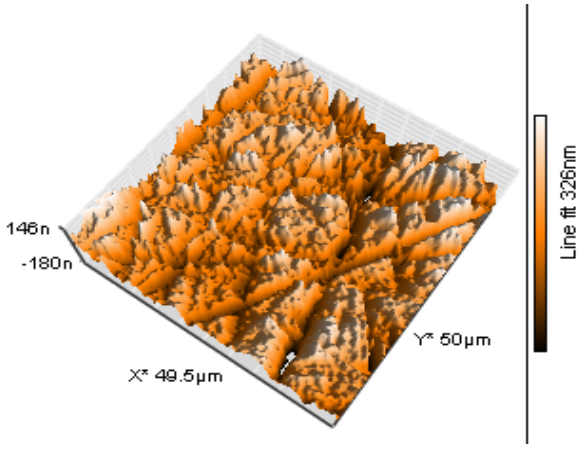

(a)

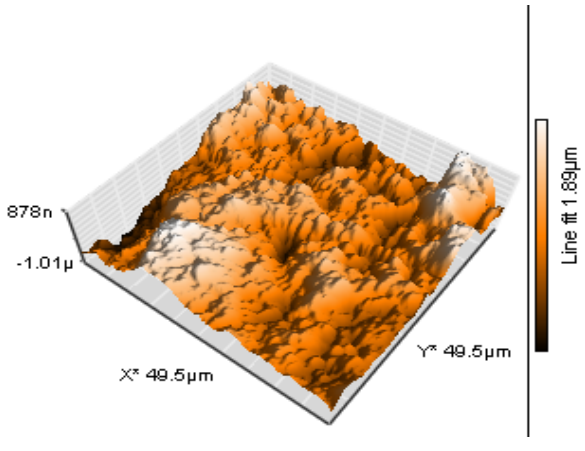

(b)

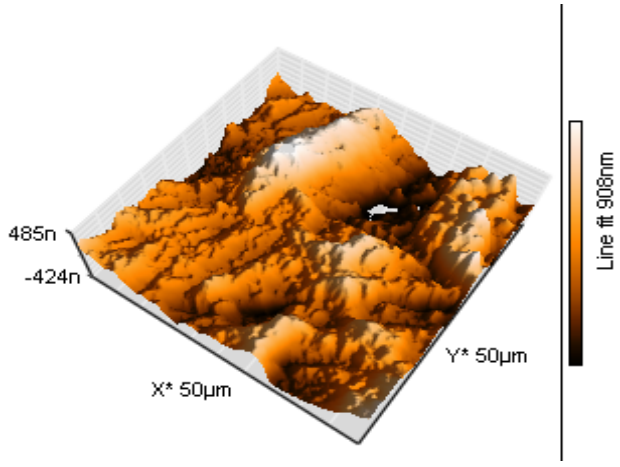

(c)

Figure 6. Typical AFM images of surface topography of (a) untreated stainless steel 316 L sample showing grinding marks with surface roughness of Sa=48.0 nm and Sy=475.8 nm, (b) plasma nitrided sample at 500 °C for 5 h in H_2:N_2=1:3 gas mixture with surface roughness of Sa=267.5 nm and Sy=2374.4 nm and (c) the sample with PECVD of silicon nitride at 400 °C for 1.5 h by the addition of 10 sccm tetraethylorthosilicate (TEOS) to the H_2:N_2=1:3 gas mixture after plasma nitriding for 5 h with surface roughness of Sa=136.1 nm and Sy=1128.4 nm.

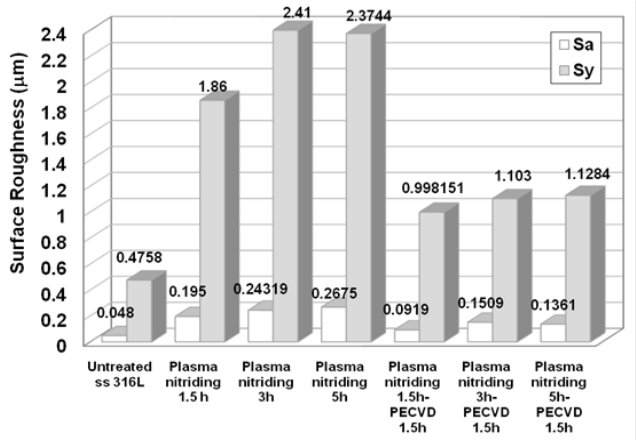

Figure 7. The bar graph shows the average surface roughness (Sa) and peak to peak surface roughness (Sy) of untreated stainless steel 316 L, plasma nitrided samples at 500 °C in H_2:N_2=1:3 gas mixture for different times and the samples treated by PECVD of silicon nitride at 400 °C for 1.5 h by the addition of 10 sccm tetraethylorthosilicate (TEOS) to the H_2:N_2=1:3 gas mixture after different times of plasma nitriding.

These can be compared to Sa and Sy for untreated material which were 48.0 and 475.8 nm respectively.It can be observed that the corresponding roughness value for PECVD treatment is considerably less than that of plasma nitriding process. Therefore it could be suggested that this PECVD treatment is promising for the reduction of surface roughness. The considerable decrease in the surface roughness of PECVD treated samples can be observed in Figure 7 in comparison with other treatments.

3.5. Friction Behavior and Wear Loss

Silicon nitride compound reduced the roughness of plasma nitrided surfaces. The decrease in the roughness facilitated the relative motion at the contact surface and in turn improved the friction behavior, such that the smoother surfaces were more suitable for exposure to sliding contact. Figure 8 compares the friction behavior of untreated, plasma nitrided and the samples deposited by pulsed dc PECVD of silicon nitride (α-Si_3N_4) compound. The friction coefficients of untreated sample reached 0.55 quickly after a short sliding distance and that of plasma nitrided samples approached 0.35 after a sliding distance of 300 m. While the friction coefficient of α-Si_3N_4 layers on PECVD treated sample was in the range of 0.1 for more than 300 m and would reach a value of about 0.3 after a much longer sliding distance of 600 m. The general decrease in the coefficient of friction of treated samples can be explained by the increase in the surface hardness of the compounds formed by plasma nitriding and PECVD of nitride layers on the stainless steel.

By increasing the hardness, the resistance of the surface layers against normal load increases resulting in lower coefficient of friction. Friction variations resulting from sliding were characterized by randomly fluctuating behavior for untreated and plasma nitrided samples (Figure 8). This variation in friction behavior has been observed by many investigators. The friction variation of the PECVD sample was very low. The friction behavior was very smooth until approximately 300 m sliding distance and gradually increased with increasing distance. The low friction value until 300 m is also related to the intrinsic low friction nature of silicon nitride (α- Si_3N_4) compound [37].

The increase in the friction value after 300 m is attributed to the removal of silicon nitride compound and exposure to other nitride phases which was approximately similar to the behavior of plasma nitrided surfaces.

Figure 9 shows a cross section profile of typical wear tracks for untreated and two treated surfaces measured by profilometer after 300 m sliding distance. We can see that the width and depth of the wear track of untreated stainless steel 316 L is ~650 µm and ~120 µm respectively. While these values changed to ~1500 µm and ~1.5 µm for the worn surface of plasma nitrided sample and to ~1600 µm and ~0.5 µm for PECVD treated sample.

It is clearly observed that the depth of wear tracks decreased considerably by special surface treatment of PECVD process.

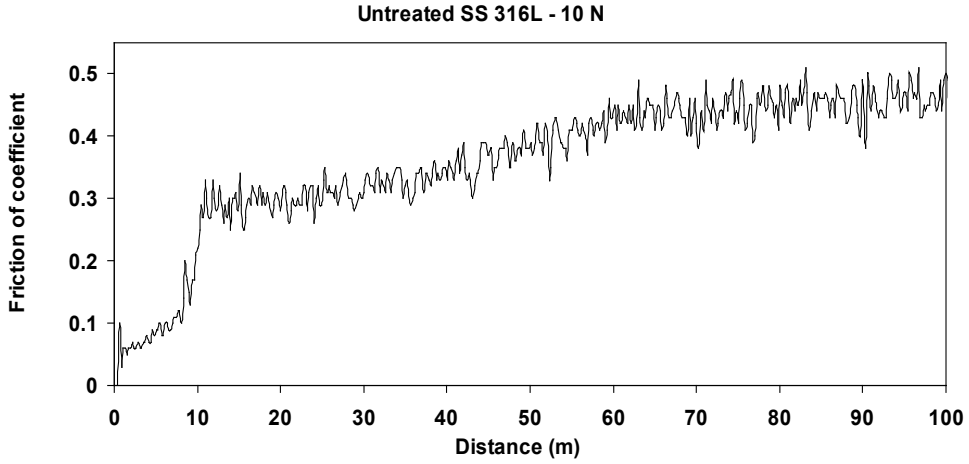

(a)

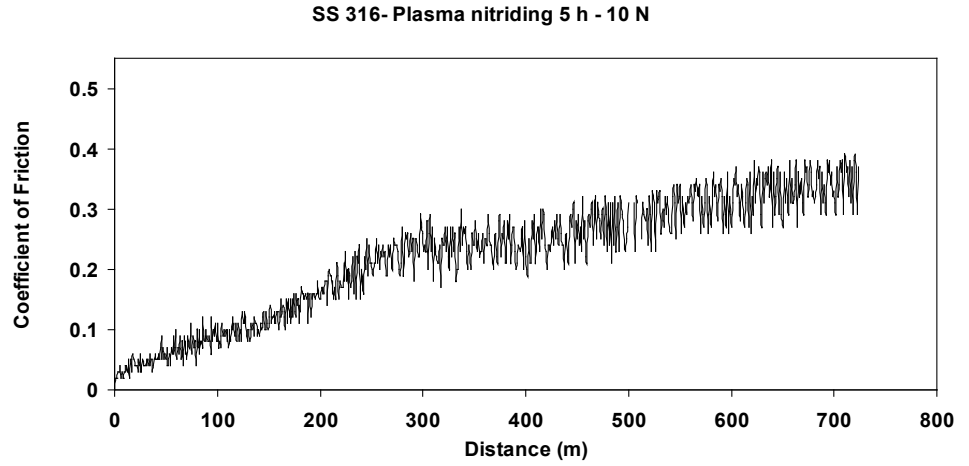

(b)

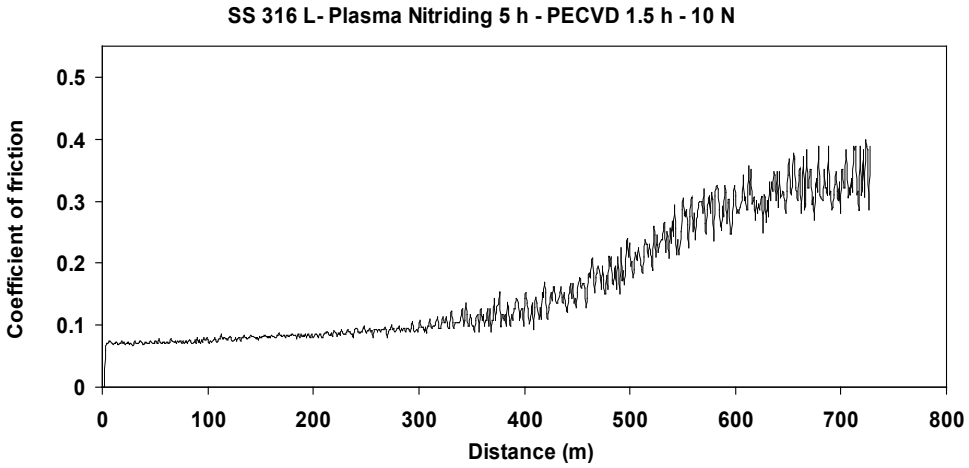

(c)

Figure 8. Friction behavior under 10 N load of (a) untreated stainless steel 316 L, (b) plasma nitrided sample at 500 °C for 5 h in H_2:N_2=1:3 gas mixture and (c) the sample treated by PECVD of silicon nitride at 400 °C for 1.5 h by the addition of 10 sccm tetraethylorthosilicate (TEOS) to the H_2:N_2=1:3 gas mixture after plasma nitriding for 5 h.

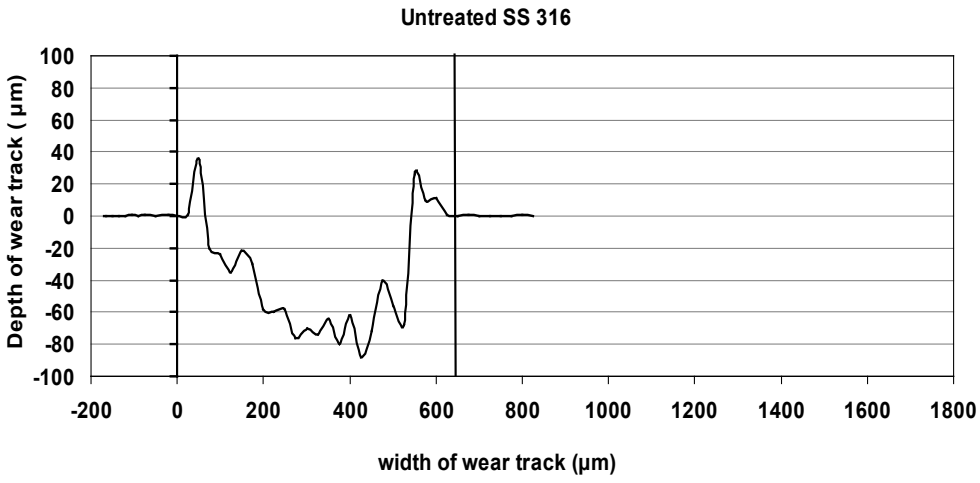

(a)

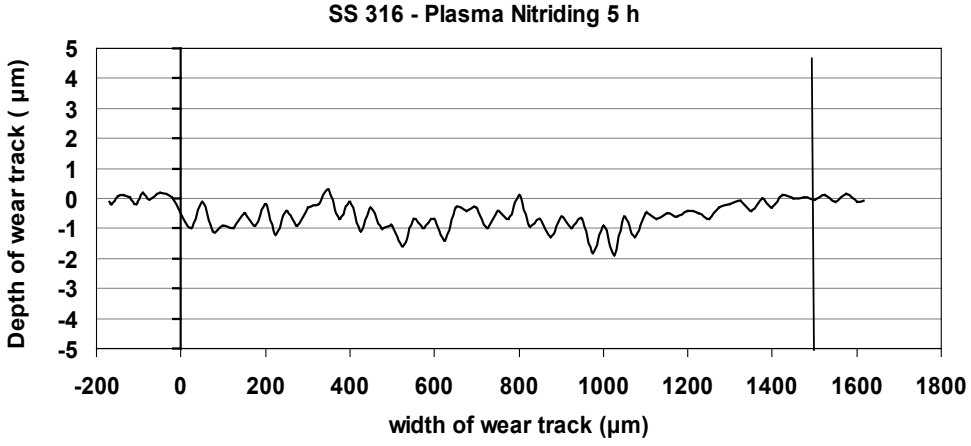

(b)

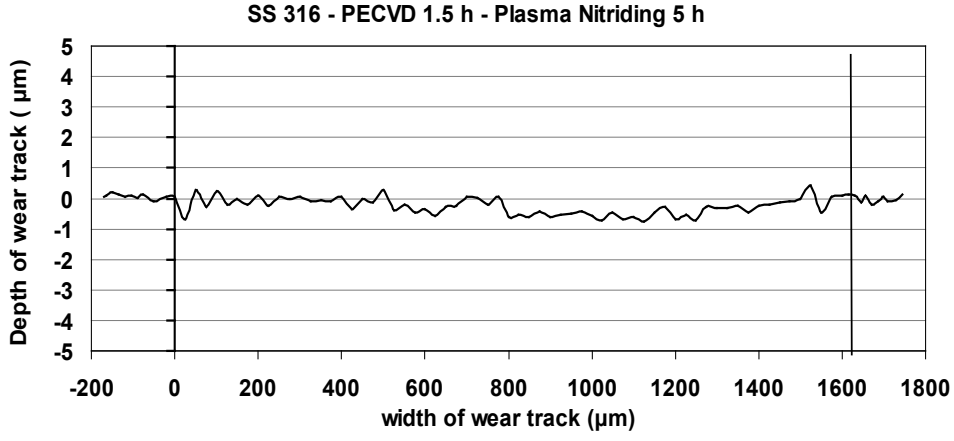

(c)

Figure 9. Profile across the wear tracks created under 10 N load after 500 m sliding distance on (a) untreated stainless steel 316L, (b) plasma nitrided sample at 500 °C for 5 h in H_2:N_2=1:3 gas mixture and (c) the sample treated by PECVD of silicon nitride at 400 °C for 1.5 h by the addition of 10 sccm tetraethylorthosilicate (TEOS) to the H_2:N_2=1:3 gas mixture after plasma nitriding for 5 h.

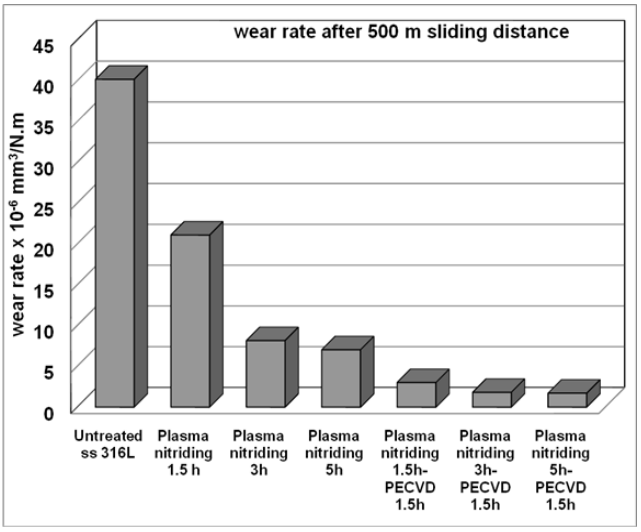

Figure 10. The bar graph shows the wear rate of untreated stainless steel 316L, plasma nitrided samples at 500 °C in H_2:N_2=1:3 gas mixture for different times and the samples treated by PECVD of silicon nitride at 400 °C for 1.5 h by the addition of 10 sccm tetraethylorthosilicate (TEOS) to the H_2:N_2=1:3 gas mixture after different times of plasma nitriding.

Dry-sliding wear rate data for untreated 316L stainless steel and treated samples are shown in Figure 10. It was observed that the wear rate of untreated stainless steel 316L was much higher than that of treated samples in all tests and at every sliding distance.

However the PECVD treatment resulted in a smoother surface. The shallow wear tracks of most treated surfaces indicated the wear resistance of the top layers and underlying surface layers supporting the top surface layers. However the wear rate of the sample plasma nitrided for 1.5 h was approximately half of that of untreated material. It decreased considerably by increasing the nitriding time. PECVD treatment decreased the wear rate of all samples significantly.

1.5 h PECVD treatment of the sample plasma nitrided for 5 h decreased the wear rate up to one order of magnitude. It was a great improvement in the wear resistance of stainless steel 316 L in comparison with that of plasma nitriding processes. This could be explained by the intrinsic wear resistance of silicon nitride (α-Si_3N_4) compound for longer sliding distances which is added to the resistance of underlying nitride layers.

The existence of Cr nitrides is mainly responsible for wear resistance or the reduction in wear loss of nitrided layers.

It has been observed that initial roughness, contact pressure, sliding velocity, material combination and environment influence the resulting values of friction coefficient and wear rate.

It may also be added that wear resistance increases by the work hardening effect that always occurs in austenitic stainless steel, even in nitrided or surface treated steels when the treated layer is broken [38].

Brittleness, low toughness and high hardness of ceramics such as silicon nitride (α-Si_3N_4) compound limit the junction-growth at asperity contacts and keep friction coefficient very low even when interlocking of asperities take a large part of friction in unlubricated pin on disk sliding in air [39].

4. Conclusions

Silicon nitride compound based on TEOS as a precursor was deposited by plasma enhanced chemical vapor deposition on plasma nitrided stainless steel 316L.

The composition, phases, hardness and mechanical properties of treated surfaces were systematically investigated.

Plasma nitriding at 500 °C for 5 h in H_2: N_2=1:3 resulted in the formation of $Fe_{2-3}N$, Fe_4N and CrN on the surfaces.

PECVD of TEOS in H_2:N_2 gas mixture after plasma nitriding created α-Si_3N_4 compound on the top surface of nitrided samples. The samples did not have considerable diffusion layers.

The thickness of plasma nitrided layers increased with increasing time up to 5 h at constant temperature and gas mixture.

PECVD treatment after plasma nitriding reduced the overall thickness of the treated layers by partial sputtering of the nitrided layers during the conversion of the top layers to silicon containing compounds.

The surface microhardness reached as high as 1700 HV0.1 after plasma nitriding at 500 °C for 5 h and 2300 HV0.1 after additional PECVD treatment for 1.5 h.

The roughness of plasma nitrided samples increased at any condition of surface treatment, while the surface roughness decreased after PECVD treatment.

The friction coefficient of treated surfaces reduced considerably. The PECVD treatment for 1.5 h after 5 h plasma nitriding had the lowest friction coefficient of nearly 0.1 until 300 m sliding distance which was a great improvement in friction behavior of treated stainless steel 316L ever made.

The high hardness or surface strengthening of the plasma nitrided and PECVD treaded layers increased the wear resistance of stainless steel 316 L up to one order of magnitude under pin on disc conditions against SAE 52100 counterface which was considerably greater than that of conventional plasma nitriding process.

Acknowledgements

The authors acknowledge Shahid Beheshti University in the Islamic republic of Iran for the financial support of this study.

REFERENCES

[1] A. Fossati, F. Borgioli, E. Galvanetto, T. Bacci. Surf. Coat. Technol., Vol.200, 3511-5513, 2006.

[2] S. Lamb, CASTI Handbook of Stainless Steel and Nickel Alloys, CASTI Publishing Inc./ASM International, Canada 2001.

[3] C. X. Li, T. Bell. Corr. Sci., Vol. 46, No.6, 1527–1547, 2004.

[4] C. Saied, A. Chala, C. Nouveau, M. A. Djouadi, L. Chekour. Plasma Process. Polym., Vol. 4, S757–S760, 2007.

[5] T. Czerwiec, H. He, G. Marcos, T. Thiriet, S. Weber, H. Michel. Plasma Process. Polym., Vol.6, No.6-7, 401–409, 2009.

[6] C. X. Li, T. Bell. Corr. Sci., Vol.48, 2036-2049, 2006.

[7] E. Rolinski. Surf. Eng., Vol.3, No.1, 35-40, 1987.

[8] N. Yasumaru. Mater. Trans. JIM, Vol.39, No.10, 1046-1052, 1998.

[9] T. Bell, Y. Sun. Heat Treatment of Metals, Vol. 29, No.3 57-64, 2002.

[10] S. Ma, J. Prochazka, P. Karvankova, Q. Ma, X. Niu, X. Wang, D. Ma, K. Xu, S. Veprek. Surf. Coat. Technol., Vol.194, No.20, 143–148, 2005.

[11] K. Miyoshi, J. J. Pouch, S. A. Altrovitz. Wear, Vol.133, 107-123, 1989.

[12] A. Batan, A. Franquet, J. Vereecken, F. Reniers, Surf. Interface Anal., Vol.40, No.3-4, 754–757, 2008.

[13] D. Li, S. Guruvenket, M. Azzi, J. A. Szpunar, J. E. Klemberg-Sapieha, L. Martinu. Surf. Coat. Technol., Vol.204, 1616–1622, 2010.

[14] G. Zhong-rong, Y. Peng-xun, F. Duo-wang, Y. Guang-hui, Tras. Nonferrous Met. Soc. China, Vol.19, s718−s721, 2009.

[15] Y. S. Li, S. Shimada. Surf. Coat. Technol., Vol.201, 1160-1165, 2006.

[16] M. Radwan, T. Kashiwagi, Y. Miyamoto. J. European Ceram. Soc., Vol.23, no.13, 2337-2341, 2003.

[17] P. Raynaud, B. Despax, Y. Segui, H. Caquineau. Plasma Process. Polym., Vol.2, No.1, 45–52, 2005.

[18] I. Vinogradov, D. Zimmer, A. Lunk. Plasma Process. Polym., Vol.4, S435-S439, 2007.

[19] M. Tsujikawa, N. Yamauchi, N. Ueda, T. Sone, Y. Hirose. Surf. Coat. Technol., Vol.193, No.1-3, 309-313, 2005.

[20] E. Arslan, M. C. Igdil, L. Trabzon, K. Kazmanl, T. Gulmez. Plasma Process. Polym., Vol.4, S717–S720, 2007.

[21] J. Wang, J. Xiong, Q. Peng, H. Fan, Y. Wang, G. Li, B. Shen. Mater. Character., Vol.60, 197-203, 2009.

[22] R. Snyders, E. Bousser, P. Amireault, J. E. Klemberg-Sapieha, E. Park, K. Taylor, K. Casey, L. Martinu. Plasma Process. Polym., Vol.4, S640–S646, 2007.

[23] Z. K. Huang, P. Greil, G. Petzow. Ceramics Inter., Vol.10, No.1, 18–22, 1984.

[24] P. Kroll, M. Milko, Z. Anorg. Allg. Chem., Vol.629, No.10, 1737–1750, 2003.

[25] R. J. Xie,† M. Mitomo, G. Dong Zhan. J. Am. Ceram. Soc., Vol. 83, No. 10, 2529-2535, 2000.

[26] F.M. El-Hossary, N. Z. Negm, A. M. Abd El-Rahman, M. Hammad. Mater. Sci. Eng: C., Vol.29, No.4, 1167-1173, 2009.

[27] J. Y. Choi, Y. T. Moon, D. K. Kim, C. H. Kim. J. Am. Ceram. Soc., Vol. 81, No. 9, 2294-2300, 1998.

[28] R. G. Duan, G. Roebben, J. Vleugels, O. Van der Biest. J. Euro.Ceram. Soc., Vol.22, no.14, 2527-2535, 2002.

[29] C. Forsich, D, Heim, T. Mueller. Surf. Coat. Technol., Vol.203, no.5, 521-525, 2008.

[30] E. De Las Heras, D. G. Santamarıa, A. Garcıa-Luis, A. Cabo, M. Brizuela, G. Ybarra, N. Mingolo, S. Bruhl, P. Corengia. Plasma Process. Polym. Vol.4, S741–S745, 2007.

[31] D. Li, S. Guruvenket, M. Azzi, J. A. Szpunar, J. E. Klemberg-Sapieha, L. Martinu. Surf. Coat. Technol., Vol.204, 1616–1622, 2010.

[32] R. Snyders, E. Bousser, P. Amireault, J. E. Klemberg-Sapieha, E. Park, K. Taylor, K. Casey, L. Martinu. Plasma Process. Polym., Vol.4, S640–S646, 2007.

[33] F.H.P.M. Habraken, A.E.T. Kuiper. Mater. Sci. Eng., Vol.R12, 123-175, 1994.

[34] A. Fossati, F. Borgioli, E. Galvanetto, T. Bacci. Surf. Coat. Technol., Vol.200, 3511-3517, 2006.

[35] Y. Zhou, X. Yan1, E. Kroke, R. Riedel, D. Probst, A. Thissen, R. Hauser, M. Ahles, H. von Seggern. Mat.-wiss. u. Werkstofftech. Vol.37, No.2, 781-789, 2006.

[36] M. Radwan, T. Kashiwagi, Y. Miyamoto. J. European Ceramic Soc., Vol.23, no.13, 2337-2341, 2003.

[37] S. Ma, J. Prochazka, P. Karvankova, Q. Ma, X. Niu, X. Wang, D. Ma, K. Xu, S. Veprek. Surf. Coat. Technol., Vol.194, No.20, 143–148, 2005.

[38] K. Kato. Mat.-wiss. u. Werkstofftech. Vol.34, No.10/11, 1003–1007, 2003.

[39] E. De Las Heras, D. G. Santamarıa, A. Garcıa-Luis, A. Cabo, M. Brizuela, G. Ybarra, N. Mingolo, S. Bruhl, P. Corengia. Plasma Process. Polym., Vol.4, S741–S745, 2007.